Pre-Layout Estimation of Individual Wire Lengths

Srinivas Bodapati and Farid N. Najm

ECE Dept. and Coordinated Science Lab.
University of Illinois at Urbana-Champaign
Urbana, Illinois 61801, USA

ECE Department
University of Toronto
Toronto, Ontario M5S-3G4, Canada

Abstract

We present a novel technique for estimating individual wire lengths in a given standard-cell-based design during the technology mapping phase of logic synthesis. The proposed method is based on creating a black box model of the place and route tool as a function of a number of parameters which are all available before layout. The place and route tool is characterized, only once, by applying it to a set of typical designs in a certain technology. We also propose a net bounding box estimation technique based on the layout style and net neighborhood analysis. We show that there is inherent variability in wire lengths obtained using commercially available place and route tools - wire length estimation error cannot be any smaller than a lower limit due to this variability. The proposed model works well within these variability limitations.

1. INTRODUCTION

In deep submicron technology, interconnect delay accounts for a significant part of signal delay. There is a need to predict interconnect delay before layout, ideally during logic synthesis. Traditionally, *wire load* models have been used during synthesis (before layout) in order to predict the capacitive load on a net. These models give the load as a function of circuit size and fanout of the net. Wire load models have been found useful for predicting the *average* load for nets with a given fanout, but cannot predict the individual load of a net [1]. Today, accurate interconnect delay is only available after layout and routing. This leads to a situation where the synthesis/layout/routing has to be repeated a number of times before the design meets the timing constraints. Problems arise when this process does not converge [2].

Therefore, a much closer interaction is needed between the synthesis and place and route tool, so that accurate wire length estimates can be provided to the synthesis engine during the technology mapping phase to achieve timing convergence. Heineken et. al [3] have proposed such a technique; they do not report individual wire lengths, instead they provide a method for obtaining wire length distributions. Hamada [4] and Pedram et. al [5] also provide models for wire length estimation. However, they also do not report individual wire lengths, instead they give one (average) wire length for all nets having the same number of pins.

Since wire length is a function of several parameters, including the algorithm used by the final placement and routing tool, we need a wire length estimation technique that can be adapted to any given placement and routing engine. Therefore, in this paper we present a wire length estimation method based on place and route tool characterization. We use structural characteristics obtained from the standard cell netlist, physical cell characteristics obtained from the standard cell library, and use linear regression to build a wire length model. We have also proposed a method for estimating the bounding box of nets with large fanouts (more than 7), which we use to estimate their wire length. Several methods have been proposed to estimate the bounding box of a net. In [6] the authors have given a brief overview of several such methods, and have proposed a net bounding box estimation based on a Uniform Pin Distribution Model. We have used net neighborhood analysis to estimate the bounding box, and the analysis in [6] to estimate the wire lengths for nets having large fanouts. We also show the inherent noise present in place and route tools (commercial) which makes it impossible to predict wire lengths beyond a certain accuracy. This paper is an expanded version of [8].

2. METHODOLOGY

The methodology used to develop the wire length model is as follows:

1. A set of standard cell verilog netlists were selected for analysis. These were placed and routed using Cadence (Silicon Ensemble) and an abstract view of the layout was created. The layouts of these design were analyzed to identify some of the salient features of the standard cell layout (discussed further in section 3), which could affect wire length. A common standard cell library was used for all the designs
2. Wire lengths for individual nets were extracted from the layout using Silicon Ensemble. Other parameters like number of cells and cell types, etc. were extracted from the netlist and standard cell library. The aim was to identify only those parameters which can be obtained without actual place and route and thus can be used to estimate individual wire lengths before layout.
3. The extracted parameters were then classified as *local* and *global*. Global parameters are those parameters which remain constant for a given design, such as the number of cells. Local parameters are those which vary within a given design and are associated with each net in the design such as the number of pins on a net, number of two pin nets in the neighborhood, etc..
4. The global parameters were used to calculate the number of standard cell rows and number of core sites in each standard cell row. A core site is the smallest space on a cell row that may be occupied by a cell; typically it corresponds to the smallest (width-wise) cell in the library, and cell widths are typically an integer multiple of the core site width. These physical parameters were then used in conjunction with the extracted local parameters to define some congestion metrics which quantify the salient features of the layout identified in step 1.
5. The congestion metrics calculated above were then analyzed to determine if some of them could be used as the significant variables of the model, i.e., if any of them correlated well with wire length and if they could be used as the basis for estimating wire length.
6. Using these congestion metrics, calculated for a set of benchmark circuits, a wire length estimation model was developed which can account for wire length variations among nets as well as across designs. This model was then verified by estimating the wire lengths of other designs and comparing the estimates with actual wire lengths obtained by the place and route tool.

3. MODEL PARAMETERS

We have used knowledge of the layout style to define placement *congestion metrics*. These metrics, along with the number of pins on the net, were then considered as the potential variables of the wire length estimation model to be constructed. These congestion metrics are based on local and global parameters, to be defined below.

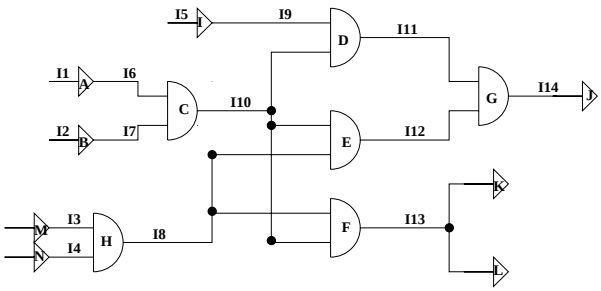

Figure 3.1 Circuit used for defining the various parameters.

3.1 Local Parameters

A key local parameter was identified as:

- *Number of pins on the net* - P_{net}. For example, the number of pins on net I10 in Fig 3.1 is 4, corresponding to cells C, D, E, and F.

Other local parameters were also identified to be useful. They are related to the structure of the *neighborhood* of the net, defined as follows (similar to [3]). The *first level neighborhood* $N_{h1}(i)$ of a net i is defined as the set of all the nets (other than i) which are connected to cells to which net i is also connected. The *second level neighborhood* $N_{h2}(i)$ of a net i is defined as $N_{h2}(i) = \bigcup_{k \in N_{h1}(i)} N_{h1}(k)$. The *neighborhood* of a net i is then defined as $N_h(i) = N_{h1}(i) \cup N_{h2}(i)$. For example, in Fig 3.1, for net I10, we have $N_{h1}(I10) = \{I6, I7, I9, I11 \dots\}$ and $N_{h2}(I10) = \{I14, I3, I4 \dots\}$. Given this, another local parameter was identified as:

- *Number of two-pin nets in the neighborhood of the given net* - N_{2net}. Since every net is connected to the output pin of a unique cell, then each of these nets corresponds to a cell, and this gives a measure of the number of cells having 2-pin nets in the neighborhood.

Likewise, we define:

- *Number of three-pin nets in the neighborhood of the given net* - N_{3net}.
- *Number of four-pin nets in the neighborhood of the given net* - N_{4net}.
- *Number of five-pin nets in the neighborhood of the given net* - N_{5net}.
- *Number of six- or more pin nets in the neighborhood of the given net* - N_{6^+net}.

Finally, we define N_{net} to be the total number of nets in the neighborhood, i.e, $N_{net} = |N_h(i)| = \sum_{k=2}^{5} N_{knet} + N_{6^+net}$

3.2 Global Parameters

The global parameters identified were:

- *Number of Cells in the design* - N_c.
- *Number of two-pin nets in the design* - N_{2agg}. Since each net corresponds to a cell, this gives us the number of cells having two-pin nets at their output.

Likewise, we define:

- *Number of three-pin nets in the design* - N_{3agg}.
- *Number of four-pin nets in the design* - N_{4agg}.
- *Number of five-pin nets in the design* - N_{5agg}.
- *Number of six- or more pin nets in the design* - N_{6agg}.

In every case, this is also the number of cells whose output is tied to a net with so many pins. Other important global parameters include:

- *Expected Row utilization factor* - U. This is a user-specified parameter which specifies how much of a row of standard cells is to be used for cell placement. It determines the size of the design. Higher row utilization factors lead to more compact designs, but routing may be difficult as the number of feedthroughs is reduced at higher U values. Placement of cells may not be possible at higher row utilization factors if the cells are very wide. This parameter was kept relatively constant in our experiments.
- *Aspect ratio of the design* - R. This is the ratio of width to height of the layout area. It was kept constant for all our experiments and its value was fixed at 1, which is a reasonable assumption. If this value is changed, wire lengths do change. This parameter can be included in our model as it is user-specified and therefore known beforehand.
- *Average Width of the Cells in the design* - W_{avg}. This is $\left(\sum_{\text{all i}} n_i W_i\right) / (N_c W_{core})$, where W_i is the width of cell i, n_i is the number of cells having width W_i, and W_{core} is the width of a core site (smallest width cell that is possible in this library). Notice that W_{avg} is thus normalized by W_{core}, and is therefore dimensionless.

There are other parameters (like timing constraints etc.) which are given to place and route engines, but we have developed our model in an unconstrained environment. By this we mean that we have not provided any delay constraints to individual nets in the layout.

4. MODEL DEVELOPMENT

The wire length model development involves the creation of a black box model of the place and route engine as a function of the congestion metrics computed using the global and local parameters. The philosophy

behind partitioning the model parameters as global and local is to capture the variation in wire lengths across designs as well as within a design. In our model, each wire length is considered to be function of P_{net} and the congestion metrics calculated for that net, to be defined below.

Our model is motivated by empirical observations, some of which will be presented below. A word is in order about the designs, the library, and the layout style that was used. The designs used for model characterization were obtained after performing placement and routing of the ISCAS and MCNC benchmark circuits shown in Table 4.1. Placement and routing was done using Cadence Silicon Ensemble. A four-metal-layer library having 1.40 micron metal pitch and 102 cells was used. This library contains the abstract cell views of the various cells (in library exchange format called LEF). The width of a core site in this library is 1.4 microns (all cell widths are integer multiples of 1.4). The standard cell height in this library was 12.60 micron. A constant U of 0.85 and $R = 1$ was used for all these designs.

4.1 Base Length

Net length is known to be a strong function of P_{net}.

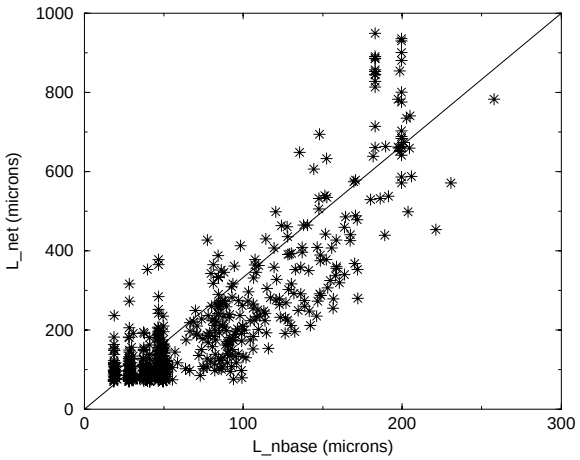

Figure 4.1 Wire length in microns v.s. L_{nbase}

Therefore, we use P_{net} to define a base wire length which along with the congestion metrics form the variables of the model. We define the base wire length as the average of the two lengths obtained by placing all the cells on the net in a single row adjacent to each other or vertically on top of each other in single column. Thus, the base length, which is denoted by L_{nbase}, is given by:

$$L_{nbase} = \frac{1}{2}\left(P_{net}H_{cell} + P_{net}\frac{W_{avg}W_{core}}{U}\right)$$

where H_{cell} is the height of a cell. Wire length exhibits a strong dependence on L_{nbase}, as shown in Fig 4.1. It was also observed that $2 * L_{nbase}$ comes very close to the actual wire length for nets with 4 to 7 pins, but not for nets with more than 7 pins. In fact, nets with more than 7 pins require special treatment. We refer to them as long nets, and we will introduce below (section 5) a bounding-box based scheme for predicting their length.

Table 4.1. ISCAS and MCNC benchmark circuits used for model characterization

Ckt	#I	#O	#Comp	#Nets	W_{avg}	N_{rows}
random8	8	1	158	280	3.65	8
s1494	14	21	674	690	3.68	18
s510	25	13	248	275	3.66	11
s832	23	18	302	327	3.62	12
c1355	41	32	434	477	4.39	16
s1196	31	24	559	592	3.66	16
c6288	32	32	2274	2309	3.82	34
c1908	33	25	411	446	4.84	16
s820o	23	15	181	206	4.45	10
s641o	52	28	116	170	4.02	7
s298o	17	12	71	90	4.35	6

4.2 Congestion Metrics

The congestion metrics used in our model were derived after analyzing several layouts. It was observed that the majority of the cells connected by two- or three-pin nets were placed close to each other and that the most common configurations were as shown in Fig 4.2a and Fig 4.2b. This occurs because, with typical placement tools based on min-cut partitioning, cells connected by two- or three-pin nets end up in the same partition, thereby reducing the partitioning cost. This also reduces the total wire length because the majority of nets in a design are two- and three-pin nets, therefore, if their corresponding cells are in the same partition, they are placed close to each other. We use this observation regarding placement of two- and three-pin nets in our derivation of congestion metrics. Basically we estimate all the possible ways of placing two and three-pin nets (cells) and then derive a measure of degrees of freedom enjoyed by the cells connected to these nets which is our congestion metric.

Consider a net i with $N > 3$ pins, and having $N_{2net} = k$ and $N_{3net} = l$. Consider the k 2-pin nets in the neighborhood. In our congestion metric, we attempt to measure the different ways of placing each of the k pair of cells, independently of each other (ie., ignoring the effect of placing one pair on the number of ways that another pair can be placed). This is a simplifying conservative assumption (which also ignores the presence of nets with more than two pins). This assumption should work better for cases of large neighborhoods (associated with high fanout, therefore usually long, nets), because in a large neighborhood the influence of one pair on the large number of ways in which another can be placed would be minimal. If the number of possible locations of placing these cells (in the configurations shown on Fig 4.2) is large (which we refer to as the degrees of freedom), then these cells may end up being spread out over a large area of the layout. This causes the N-pin net to be also spread out over a large area, so that it becomes a long net. This behavior has been observed in practice, and motivates our definitions of the congestion metrics given below. It should be noted however that while analyzing two-pin nets we ignore the presence of three-pin nets because in our empirical study of various layouts, the placement of cells with two-pin nets was not influenced by the presence of three-pin nets, i.e. if a cell has both two- and three-pin nets, in the majority of cases it would be placed close to the cell connected by a two-pin net. But when we analyze the three-pin nets we do take into account the presence of two-pin nets, because the placement configuration of three-pin nets (shown in Fig 4.2b) includes that of two-pin nets (this is an empirical observation from the layout).

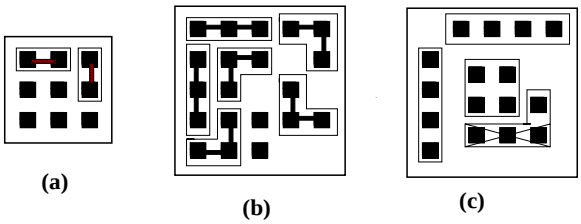

Figure 4.2 Possible placement

configurations for 2, 3 and 4 pin nets.

We start with a congestion metric that is related to 2-pin nets, which we call *2-pin congestion*, denoted by P_{2con}, and which is defined as follows. Consider that the sum total of the lengths of all the rows in the standard-cell layout can be computed in two ways. One way is the obvious $N_c W_{avg} W_{core}/U$, where W_{core} is the width of a core site. Another way is $N_{rows}\,(RN_{rows}H_{cell})$, where N_{rows} is the number of standard cell rows in the design. The second expression is true because R is given by row length divided by $N_{rows}H_{cell}$. Equating these two expressions yields $N_{rows} = \sqrt{\frac{N_c W_{avg} W_{core}}{H_{cell} U R}}$. The number of core sites would, therefore, be $N_{core} = N_{rows} H_{cell} R/W_{core}$. As mentioned previously, based on empirical observations, we will assume that 2-pin nets can only be placed in either of the two configurations shown in Fig 4.2a. If only the horizontal configuration is used, then one can show that the number of possible ways to lay out a 2-pin net is given by

$$P_{2conb} = \left(\frac{N_{core}}{W_{avg}} - 1\right) U N_{rows}$$

This expression can be derived from the fact that, N_{core}/W_{avg} is the average number of cells which can be placed in a single standard cell row. Thus $\left(\frac{N_{core}}{W_{avg}} - 1\right)$ represents the possible ways of placing two cells in a horizontal row adjacent to each other. We can imagine the two cells as a single group and slide this group over a horizontal grid of width W_{avg}. Since there is a row utilization factor U, the number of possible placements in a single row reduces by this factor. If we consider the fact that the number of rows is N_{rows}, we get P_{2conb}, which is the number of ways of placing cells connected by a 2-pin net, adjacent to each other. If only the vertical configuration is used, then the number of ways to layout a 2-pin net is given by

$$P_{2cona} = \frac{(N_{rows} - 1) U N_{core}}{W_{avg}}$$

$N_{rows} - 1$ is the number of possible ways of placing two cells on top of each other in a single vertical grid of size H_{cell}. Since there are N_{rows} grid points, we have $N_{rows} - 1$ possible ways of placing two cells on top of each other in a single file. Since there are UN_{core}/W_{avg} such files in the layout, we get P_{2cona} To factor in both possibilities, we simply take the sum $(P_{2cona} + P_{2conb})$, just to keep our complexity measures simple. Since the design has a total of N_{2agg} 2-pin nets, the number of possible ways to layout each of them is given by $(P_{2cona} + P_{2conb})/N_{2agg}$ (this is an approximation, because we ignore the presence of other cells). This, in a sense, is a measure of the degrees of freedom enjoyed by each 2-pin net, assuming all of them are placed independent of each other, disregarding the presence of other cells. We ignore the effect of other cells because it was observed in various layouts that cells with two-pin nets are placed close to each other, independent of the presence of other cells. For a net i with N_{2net} 2-pin nets in the neighborhood, the number of possible locations in which the cells tied to these 2-pin nets can be placed (in the configurations of Fig. 4.2a), is a measure of how spread out these 2-pin nets (and therefore the neighborhood cells themselves) may be on the layout surface. Based on this, we define our first congestion metric, related to 2-pin nets in the neighborhood, as $P_{2con} = (P_{2cona} + P_{2conb})N_{2net}/N_{2agg}$. We will refer to this as the *2-pin congestion*. Typical dependence of wire length on P_{2con} shown in Fig. 4.3.

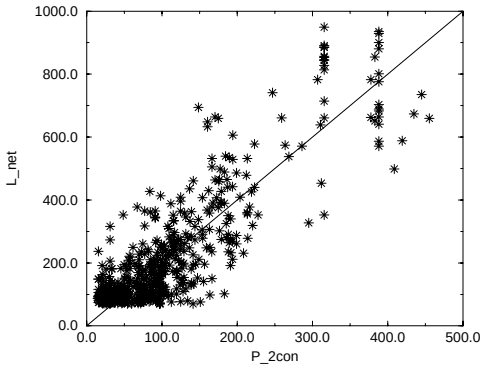

Figure 4.3 Wire length in microns v.s. P_{2con}

In a similar way, for three-pin nets we define *3-pin congestion*, denoted by P_{3con},

$$P_{3con} = \frac{(P_{3cona} + P_{3conb} + P_{3conc})(N_{3net} + N_{2net})}{N_{2agg} + N_{3agg}}$$

where:

$$P_{3conb} = \left(\frac{N_{core}}{W_{avg}} - 2\right) UN_{rows}$$
$$P_{3cona} = \frac{(N_{rows} - 2)UN_{core}}{W_{avg}}$$
$$P_{3conc} = 4\left(\frac{N_{core}}{W_{avg}} - 1\right) U(N_{rows} - 1)$$

P_{3cona} gives the number of possible ways of placing three cells connected by a net adjacent to each other. P_{3conb} is the number of possible ways of placing three connected by a net vertically on top of each other. Both these equations have been derived in a similar manner as P_{2cona} and P_{2conb}. P_{3conc} gives the possible ways of placing a triplet of cells in rest of the four configurations shown in Fig 4.2(b). This can be derived by sliding each of those four placement configurations both vertically and horizontally along and across the standard cell rows. $\left(\frac{N_{core}}{W_{avg}} - 1\right) U(N_{rows} - 1)$ is the possible ways of placing a triplet of cells in each of the configurations shown in Fig. 4.2(b). Since there are four such configurations we get P_{3conc} Since all these possible placement configurations include the placement of cells connected by 2-pin nets, we need to take into account their presence also. The design has a total of $N_{2agg} + N_{3agg}$ 2-pin and 3-pin nets; the number of possible ways to layout each of them is given by $(P_{3cona} + P_{3conab} + P_{3conc})/(N_{2agg} + N_{3agg})$. Thus we get P_{3con}, if we consider the number of 2-pin and 3-pin nets in the neighborhood of a given net.

These computations take into account (approximately) the presence of 2-pin nets [6]. We need to take into account the presence of 2-pin nets because, all the placement configurations of 3-pin nets includes the placement of 2-pin cells, and it was also observed in layouts that 2-pin nets were dominating over 3-pin nets as far as placement is concerned, hence 2-pin nets were considered independent of 3-pin nets. It may seem that we are duplicating the effect of 2-pin nets here, but we need to consider their influence separately too (P_{2con}) because they have an exclusive effect on wire length independent of the presence of 3-pin nets. The influence of 3-pin nets in the presence of 2-pin nets cannot be independent because the placement engine will try to optimize 2-pin nets over 3-pin nets, if we have both 2-pin and 3-pin nets in the same partition.

Similarly we define *4-pin congestion* P_{4con}, *5-pin congestion* P_{5con} and *6-pin congestion* P_{6con}. In *4-pin congestion* we consider 4-pin nets in the neighborhood. In *5-pin congestion* we consider 5-pin nets, but in *6-pin congestion* we consider nets with 6 or more pins. Of these metrics, it was found that *4-pin congestion* is dominant (in terms of how it affects wire-length) in comparison to the other two variables, though its influence is less compared to 2- and 3-pin congestion. This is why we simply lumped all nets with six or higher pins into a single measure.

For 4-pin congestion, only the three basic configurations shown in Fig. 4.2c were considered. For 5 and 6 pin congestion metrics, we do not consider any possible placement configurations. These three congestion metrics are defined as:

$$P_{4con} = \frac{(P_{4cona} + P_{4conb} + P_{4conc})\,(N_{2net} + N_{3net} + N_{4net})}{(N_{2agg} + N_{3agg} + N_{4agg})}$$

where:

$$P_{4cona} = \frac{(N_{rows} - 3)\,UN_{core}}{W_{avg}}$$
$$P_{4conb} = \left(\frac{N_{core}}{W_{avg}} - 3\right) UN_{rows}$$
$$P_{4conc} = (N_{rows} - 1)\left(\frac{N_{core}}{W_{avg}} - 1\right) U$$

$$P_{5con} = \left(N_{rows} \frac{N_{core}}{W_{avg}} U - (N_{2agg} + N_{3agg} + N_{4agg}) \right) \frac{N_{5net}}{N_{5agg}}$$
$$P_{6con} = \left(N_{rows} \frac{N_{core}}{W_{avg}} U - (N_{2agg} + N_{3agg} + N_{4agg}) \right) \frac{N_{6^+net}}{N_{6agg}}$$

P_{4cona} and P_{4conb} are the ways of placing four cells adjacent to each other in a single row or on top of each other in a single file. P_{4conc} is gives the possible ways of placing four cells in the configuration shown in Fig. 4.3(c).The expression for P_{4con} can be obtained after an analysis similar to that for 3-pin and 2-pin congestion metrics. The only difference is that the placement configurations considered for 4-pin nets also include the configuration for 2-pin and 3-pin nets; thus we have to take into account their influence also.

We have to consider the influence of five or more pin nets in the neighborhood of a given net, say i, because the bounding box for i would contain the cells driving these five or more pin nets. Since compared to two, three and four pin nets, there aren't many five or more pin nets, there impact on wire length varies a lot. Moreover there weren't any fixed patterns of placement observed for cell connected by these nets (because most of the cells connected by such nets invariably have a two or three pin net connecting them). Therefore, we did not consider any placement configurations for the cells connected by these nets. Thus $\left(N_{rows} \frac{N_{core}}{W_{avg}} U \right)$ is total number of placement sites in layout. If we subtract the number of cells connected by 2-, 3- or 4-pin nets from these, then the remaining core sites are available for placing these cells. Thus P_{5con} gives the possible ways of placing each of the N_{5agg} cells over the remaining core sites, which when multiplied by N_{5net} measures the degree of freedom enjoyed by the cells in the neighborhood of net i. Since the influence of both N_{5net} and N_{6^+net} was not very significant (Table 4.2), P_{6con} was derived independently of the influence of N_{5net}, but the arguments remain identical, except that instead of N_{5net} we use N_{6^+net}.

4.3 One More Variable

Finally, one more variable was found to be required in order to reflect the presence of a large number of 2-pin nets in some cases. Cells that are joined by 2-pin nets are placed close together in order to optimize the total wire length, and if there is a large number of them (which is typically the case) they can end up being "in the way" and can cause the layout of a net to result in bigger length. Basically, we need a measure of the number of 2-pin nets that may end up being placed among (i.e. in the same general layout area as) cells that belong to the neighborhood of the net in question. We propose to use a measure N_{2oth}, defined by $N_{2oth} = (N_{2agg} - N_{2net}) \frac{N_{net}}{N_c}$. The reasoning behind this definition, and the reason this measure is useful, is as follows. Consider that each net corresponds uniquely to a cell in the netlist, the cell that drives it. For a given net, $N_{2agg} - N_{2net}$ gives the total number of cells in the design that drive 2-pin nets that are outside the neighborhood of this net. A certain fraction of this total will end up being placed "in the way" and we estimate this fraction as the ratio of the size of the neighborhood to the size of the whole design. Thus, this gives a measure of how many remaining 2-pin nets or cells (which are not in the neighborhood) may end up being placed among those neighborhood cells. Typical dependence of wire length on N_{2oth} is shown in Fig. 4.4.

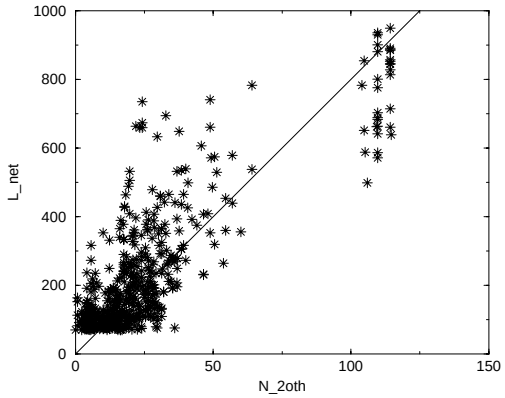

Figure 4.4 Wire length in microns v.s. N_{2oth}

But before using these parameters in our model, we must ensure that these variables have a significant impact on the wire length. In statistics there are several ways to measure the statistical significance of the proposed variables, we use the simplest measure the correlation coefficient. The correlation coefficient, ρ, between two variables x, y is defined as,

$$\rho = \frac{\sum_{i=1}^{n}(x_i - \overline{x})(y_i - \overline{y})}{\sigma_x \sigma_y}$$

$$\sigma_x = \sqrt{\frac{\sum_{i=1}^{n}(x_i - \overline{x})^2}{n-1}}$$

$$\sigma_y = \sqrt{\frac{\sum_{i=1}^{n}(y_i - \overline{y})^2}{n-1}}$$

where $\overline{x}$ and $\overline{y}$ are the mean of x and y respectively. The correlation coefficient of each of these variables with respect to wire length is shown in Table 4.2, for some designs. it can be seen that variables in the first four columns, and the last column have a significant correlation with the actual wire length. The other two variables which are contributions due to neighboring cells connected to more than 5 pins, do not have a very regular impact. For example in c6288 there are no such nets, and in most of the cases, there aren't many such nets in the neighborhood. But even if they are present their impact on wire length is not very regular. Since in some cases the correlation is more than 60% we have included them in our model (only as a linear term). Since 2- and 3- pin nets are in majority their impact on the nets in their neighborhood is significant. The negative correlation for one of the designs can be ignored as it is very low, and it doesn't have a large number of such nets, to make that statistic significant, basically it can considered an outlier. The table also shows that the correlation coefficient of 2-pin cells which are not in the neighborhood also has a significant impact on the wire length of individual nets.

Table 4.2. Correlation between wire length and various parameters used in the model.

Ckt	L_{nbase}	P_{2con}	P_{3con}	P_{4con}	P_{5con}	P_{6con}	N_{2oth}
c6288	.9645	.9486	.9419	.9272	0	0	.9502
s1494	0.8931	0.8107	0.8107	.7793	.7014	.6697	.7540
s1196	.7989	.7562	.7531	.7572	.4831	.6693	0.7347
s832	.8344	.7642	.7783	.7677	.4418	.5034	.6741
c1355	.8525	.7335	.7332	.7058	.5166	-0.0172	0.5678
s510	.8112	.7132	.7010	.6864	.4617	.3404	.5568
c1908	.9073	.7915	.7984	.7344	.2326	.4660	.7744

4.4 The Model

The wire length model is expressed as a function:

$$L_{net} = f\left(L_{nbase}, P_{2con}, P_{3con}, P_{4con}, P_{5con}, P_{6con}, N_{2oth}\right)$$

Since our intention is to develop a model that is closely coupled to a given place and route engine, and at the same time adaptable to different place and route tools, we developed the model for L_{net} by fitting a general polynomial function. It was found that a general second order or cubic polynomial is sufficient. However, in order to reduce the complexity of this 7-variable model, we ignored all cross-product terms except those with L_{nbase}, since L_{nbase} was found to be the most significant variable. For a cubic polynomial, this reduces the number of terms from about 40 to just 20, without significantly impacting the quality of the fit. The actual equation used to model the wire length is given by:

$$\begin{aligned} L_{net} = {} & P(0)\,x_1 + P(1)\,x_1^2 + P(2)\,x_2 + P(3)\,x_2^2 \\ & + P(4)\,x_2^3 + P(5)\,x_3 + P(6)\,x_3^2 + P(7)\,x_3^3 + P(8)\,x_4 + P(9)\,x_4^2 \\ & + P(10)\,x_5 + P(11)\,x_6 + P(12)\,x_7 + P(13)\,x_7^2 + P(14)\,x_1x_2 + P(15)\,x_1x_3 \\ & + P(16)\,x_1x_4 + P(17)\,x_1(x_5 + x_6) + P(18)\,x_1x_7 + P(19) \end{aligned}$$

where $x_1, x_2, x_3, x_4, x_5, x_6$ and x_7 are $L_{nbase}, P_{2con}, P_{3con}, P_{4con}, P_{5con}, P_{6con}$ and N_{2oth} respectively. The coefficients of the polynomial are obtained using least squares fitting, based on the circuits in Table 4.1.

5. NET BOUNDING BOX ESTIMATION

The model presented so far works well for the majority of nets, but it does not apply very well to nets with large fanouts (more than 7). Since nets with fewer pins are routed first, these long nets end up being spread over a much larger area on the layout, than it would be for nets with less fanout. Thus, we make special-case treatment, by first estimating the dimensions of the *bounding box* for each of these nets. In the following, we will present ways of estimating the area of the bounding box, then its width and height, then the net length.

5.1 Area Of The Bounding Box

If N_{box} is the number of cells in the bounding box, then one way of estimating its area is $B_{boxarea} = N_{box} W_{avg} W_{core} H_{cell} / U$. The cells in the bounding box will certainly include those in the first level neighborhood. In addition, this being a long net, most of the nets in the second level neighborhood will also belong to the bounding box, because they will typically be placed first. Therefore, we will simply consider that the neighborhood (containing a total of N_{net} cells) belongs to the bounding box.

Apart from the cells in the neighborhood, other cells (most importantly, those driving two or three pin nets) could be in the bounding box as well. We will actually focus only on cells having 2 and 3-pins, because these cells are placed first, as mentioned previously, and they end up being "in the way" as mentioned in section 4.3. Thus we will estimate the total number of cells in the bounding box as:

$$N_{box} = N_{net} + N_{2oth} + N_{3oth}$$

where N_{2oth} is same as defined in section 4.3, and N_{3oth} is similarly defined as:

$$N_{3oth} = (N_{3agg} - N_{3net}) \frac{N_{net}}{N_c}$$

5.2 Dimensions Of The Bounding Box

Now we can estimate the dimensions of the bounding box if we take into account a simple observation made while analyzing the results of the P&R tool. It was found that in majority of cases each cell of a large fanout net was placed in a different row. Thus if P_{net} is the number of pins on a net, then the net would span at least P_{net} rows of the design (if $P_{net} \leq N_{rows}$), thus we assume this to be the height of the bounding box. We found this to be a good approximation in practice. Thus, if $P_{net} \leq N_{rows}$, we estimate the height of the bounding box as $B_{boxht} = P_{net} H_{cell}$. If $P_{net} > N_{rows}$ then the number of standard cell rows limits the height of the bounding box and it becomes $B_{boxht} = N_{rows} H_{cell}$. With this, the width of the box becomes simply $B_{boxwd} = \frac{B_{boxarea}}{B_{boxht}}$.

5.3 Wire Length Estimation

Finally, given the bounding box dimensions, we estimate the net length. In [7], the expected cost (total net length) of a Rectilinear Steiner Minimal Tree (RStMT) routing of a given net is explored, for various scenarios. It is shown that, when P_{net} is large, this length is given by $\sqrt{B_{boxarea} P_{net}}$, provided that the aspect ratio ($R_{box} = \frac{B_{boxwd}}{B_{boxht}}$) is less than 1. They have also shown that when $R_{box} > 1$, then the length deviates substantially from $\sqrt{B_{boxarea} P_{net}}$.

We use this result in our estimation. When $R_{box} \leq 1$, we compute the length as $\sqrt{B_{boxarea} P_{net}}$. When $R_{box} > 1$, we will use the half-perimeter length of the bounding box as a measure of length, i.e., $B_{boxwd} + B_{boxht}$. The comparisons based on this approach will be shown in section 7 (Figure 7.7).

6. NOISE IN ACTUAL WIRE LENGTH

The model obtained after characterization on a set of designs was used to estimate the wire lengths for a *different* set of designs. The estimates were found to be good in some cases but also very poor in some

other cases. Upon analysis of the Verilog netlists, we found that the naming convention followed for the cell names was different from what was used in the circuits used in the characterization runs. If the names were changed, agreement became very good! Likewise, individual wire lengths were found to depend on other parameters which are not strictly under user control. Some of these parameters were the *names of the cells*, the *order of the cells*, and the *names of the nets*. Changes in the above parameters lead to changes in the individual wire lengths, even though the average wire length remains relatively constant. The most plausible reason for this might be that the data structures for place and route tools are built using the string variables (say cell names,) and, depending on the strings, the organization of data changes under different naming conventions leading to a different placement. This does not represent a problem with the place and route tool, because multiple placement solutions may be equally good, due to the fact that the tool aims to minimize the *total* wire length. We consider such variations in wire length as *noise* because one cannot control this inherent variability of a P&R engine and cannot possibly hope to account for it in the general case. A typical example of this behavior is show in Fig. 6.1, where the noise in the wire lengths in alu2o is shown. In this figure, both axes represent extracted wire lengths from actual layouts done with different cell names.

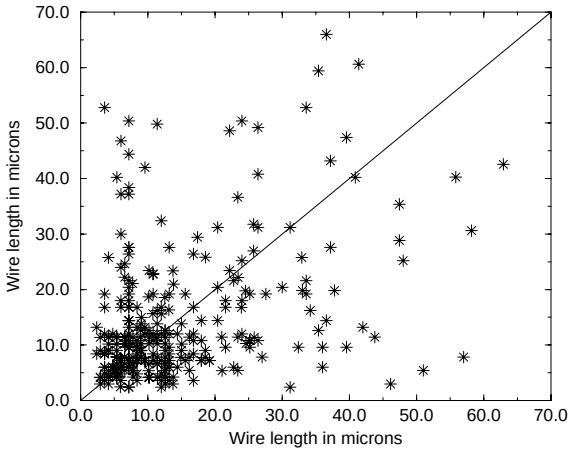

Figure 6.1 Almost random variations in wire lengths less than 70 microns due to changes in cell name

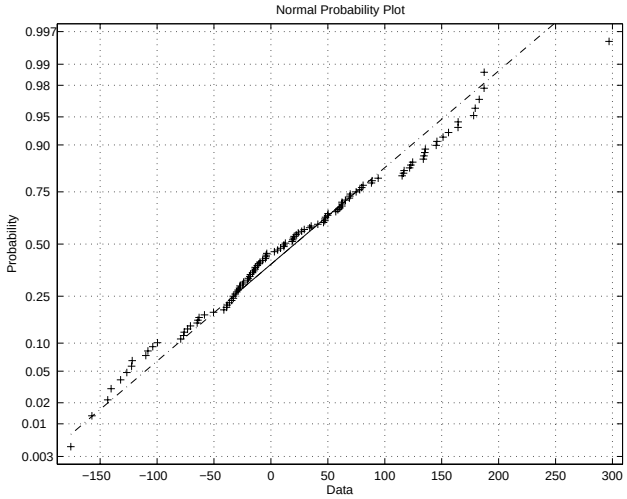

Figure 6.2 Normal plot of the residues for long wires.

Table 7.1. ISCAS and MCNC benchmark circuits used in Figs.7.1–7.7

Circuit	#Inputs	#Outputs	#Cells	#Nets	W_{avg}	N_{rows}
alu2o	10	4	368	380	3.65	13
s1238o	31	22	331	364	4.55	14
apex6o	135	85	775	912	3.52	19
frg2o	142	109	451	595	4.39	16
x3o	135	89	792	929	3.54	15
random10_325	10	1	487	499	3.73	15
c1355	41	32	434	477	4.39	16
c2670	157	64	425	579	4.41	16
c5315	178	123	1009	1264	4.76	28
s1494	14	21	674	690	3.68	18

Variations (noise) in wire length due to the above mentioned parameters were very strong for wire lengths less than 70 microns (see Fig 6.1, for alu2o). Hence, we consider that estimation for short wires is extremely difficult. Fortunately, it is more important to estimate wire length accurately on long wires. Thus, we have applied our model to only the set of wires that are longer than 70 microns. Even for wire lengths above 70 micron, a change in cell names does cause some variation in individual wire length, as shown in Figs. 7.1–7.7. Thus, individual wire lengths cannot be estimated beyond a certain accuracy - the *noise floor* depends on the specific place and route tool. Thus, the actual wire length obtained for various nets in a given design can be considered to be consisting of two parts, given by

$$L_{actual} = L_{design} + \eta$$

where L_{design} is that part of the actual wire length, which is independent of the netlist format (like cell names, order of the netlist etc.), and η is that part which depends on netlist format. Now any wire length estimation model (except the actual algorithm used in the placement and routing engine), can model L_{design} and cannot model η if it is random. In order to verify that this variation is indeed random, we analyzed the differences (residues) in actual wire lengths due to changes in cell names, and order of the Verilog netlist, for long wires. In this regard, the residues were also plotted on a normal probability plot. The purpose of a normal probability plot is to graphically assess whether the sample data (in this case the residues) come from normal distribution. If the data are normal the plot will be linear. The normal plot of the residues (Fig 6.2) shows that the majority of points do lie on straight line. Thus the variations in actual wire length due to changes in netlist format, can be modeled as a normal distribution, with some mean and variance. But since our current objective is to estimate wire length, we have not analyzed the distribution of the residues over several designs. But Fig 6.2 shows that variations in wire length due to changes in netlist format are indeed random and hence cannot be accounted for in a wire length estimation model.

7. EXPERIMENTAL RESULTS

The above modeling technique was implemented in a tool called WLE (wire length estimator). The wire length estimates obtained using our model, for wire lengths above 70 micron, are within the noise limit inherent to the place and route system, as shown in Figs. 7.1–7.14 and Table 7.2. The plots shown in Fig 7.1–7.15 were obtained from ISCAS and MCNC benchmark circuits shown in Table 7.1. Since the model is based on regression we have also included in Table 7.2 the *coefficient of determination*, R^2_{reg}, a very popular statistic used to measure the proportion of variability of the dependent variable explained by regression on predictor variables. R^2_{reg} is given by

$$R^2_{reg} = \frac{SS_{reg}}{SYY}$$

where SS_{reg} is the sum of squares due to regression and SYY is the corrected sum of squares of the actual wire lengths, given by

$$SYY = \sum (y_i - \bar{y})^2$$

$$SS_{reg} = SYY - \sum (y_i - \hat{y_i})^2$$

where y_i is the actual wire length and $\hat{y_i}$ is the estimated wire length, and $\bar{y}$ is the mean of y_i.

In Fig 7.7 we have shown the wire length estimates for nets having more than 7 pins using the bounding box based wire length estimation technique. All the designs in Table 7.1 were used to get this plot. The library used was the same library described in section 4. Figs. 7.8–7.13 show the distribution of the relative error between the predicted wire length and the actual wire length. They also include the distribution of the relative difference between actual wire lengths obtained after changing the cellnames and the order of the cells in the netlist.

In order to verify that our model can be used with a different library, we mapped some of the benchmark circuits to a different library and generated some results. Fig 7.14 and Fig 7.15 were obtained using this new library. It is a three-metal-layer library with 1.20μ metal pitch. The standard cell height in this library was 10.80μ and the width of a core site was 1.2μ. The relative error distribution and noise distribution for wirelength using this library is shown in Fig 7.16 and Fig 7.17. The errors are slightly larger with the different library, but the noise is also larger, and overall the approach works well within the noise limits on both libraries.

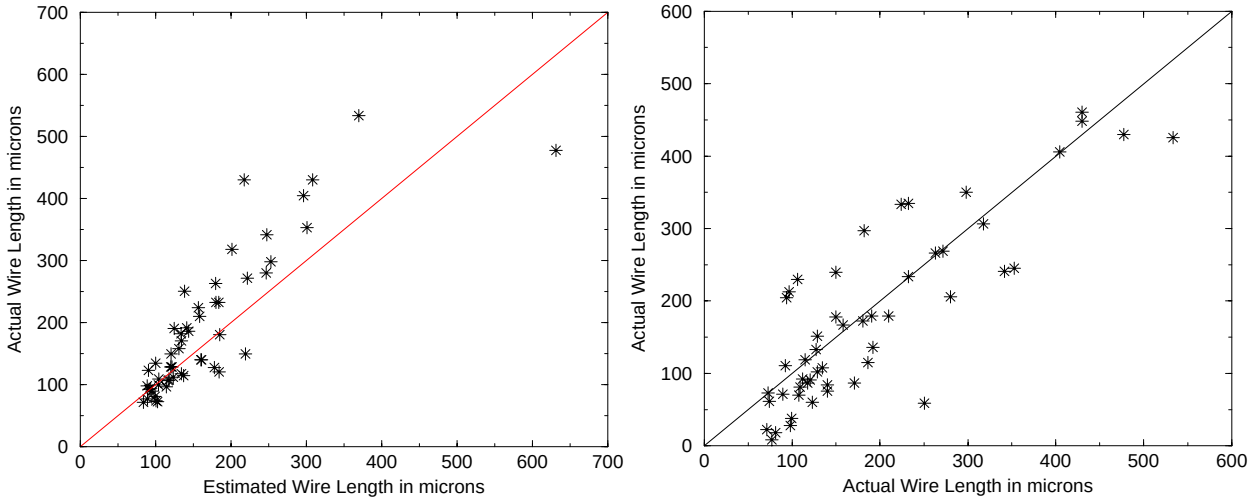

(a) (b)

Figure 7.1 For alu2o, (a) actual vs. estimated wire length using WLE, and (b) inherent noise in the actual wire length.

8. CONCLUSION

We have presented a model for estimating individual wire lengths. A significant aspect of this technique is that it can be adapted to a given place and route engine (in this case Silicon Ensemble) by a one-time process of characterization. Since the wire length estimation technique is based on creating a black box model of the place and route engine by characterization, it might be possible to create similar models for other place and route systems. Thus, we have proposed a technique which can be used to provide a close interaction between the synthesis stage and the final place and route which is needed in order to achieve timing convergence. Moreover, we have shown that there is an inherent noise in place and route tools which causes variations in the wire length for the same netlist when some insignificant parameters in the netlist file are changed, which makes it difficult to predict individual wire lengths, most notably for short wires, and to a lesser extent for long wires.

9. REFERENCES

[1] H. Kapadia and M. Horowitz, "Using partitioning to help convergence in the standard-cell design automation methodology," *Design Automation Conference*, pp. 592–597, June 1999.

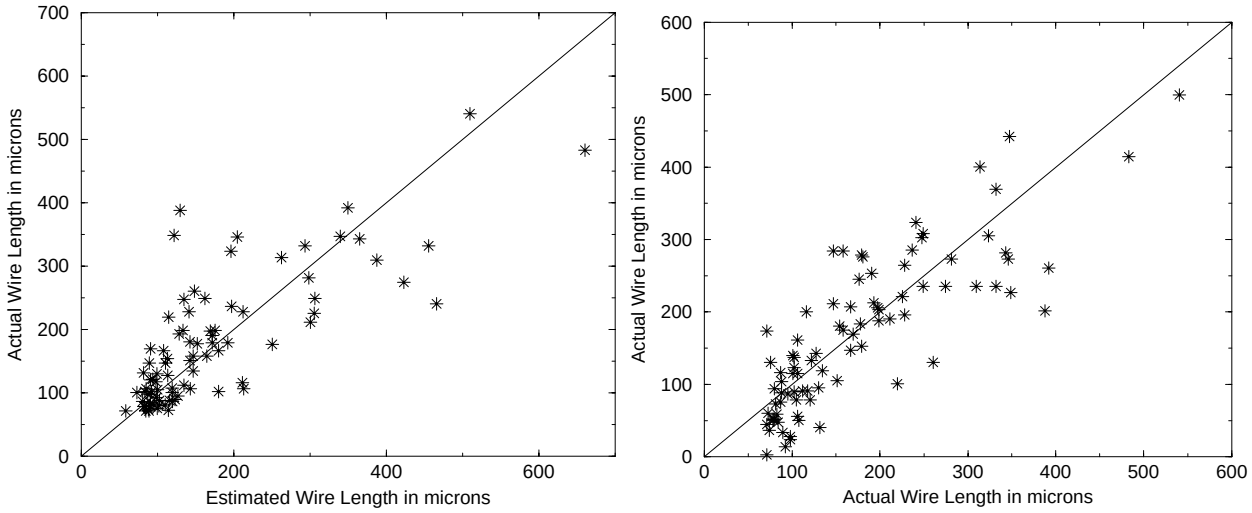

(a) (b)

Figure 7.2 For s1238o, (a) actual vs. estimated wire length using WLE, and (b) Inherent Noise in the actual wire length.

Table 7.2. Average estimation error v.s. average noise in the system

Circuit	Avg Est. Error	R^2_{reg}	Avg Noise
alu2o	21.75%	0.7523	33.76%
s1238o	26.46%	0.6451	31.11%
apex6o	22.15%	0.8397	42.48%
frg2o	27.05%	0.8356	25.07%
x3o	22.53%	0.8547	47.00%
random10_325	26.55%	0.7120	35.55%
longwires	31.00%	$NA^{\dagger}$	26.92%

† longwires estimated using bounding box method hence R^2 not defined

[2] Paul McLellan, "The radical changes wrought by deep submicron IC technology," *EDA Today Summary Report*, vol. 1, no. 6, June 1995.

[3] H. T. Heineken and W. Maly, "Standard cell interconnect length prediction from structural circuit attributes," *Proc. Custom Integrated Circuits Conference*, pp. 167–170, May 1996.

[4] T. Hamada, C.-K. Cheng and P. M. Chau "A wire length estimation technique utilizing neighborhood density equations," *IEEE Transactions on Computer-Aided Design*, vol. 15 pp. 912–922, August 1996.

[5] M. Pedram and B. T. Preas, "Interconnection length estimation for optimized standard cell layouts," *International Conference on Computer Design*, pp. 390–393, October 1989.

[6] S. Bodapati, "Pre-layout estimation of individual wirelengths," MS Thesis, Univ. Of Illinois, Urbana, IL, USA, 2000.

[7] A. E. Caldwell, A. B. Kahng, S. Mantik, I. L. Markov and A. Zelikovsky, "On wirelength estimations for row-based placement," *IEEE Transactions on Computer-Aided Design*, pp. 1265–1278, Sep 1999.

[8] S. Bodapati and F. N. Najm, "Pre-layout estimation of individual wire lengths," *ACM International Workshop on System-Level Interconnect Prediction*, pp. 93–98, April 2000.

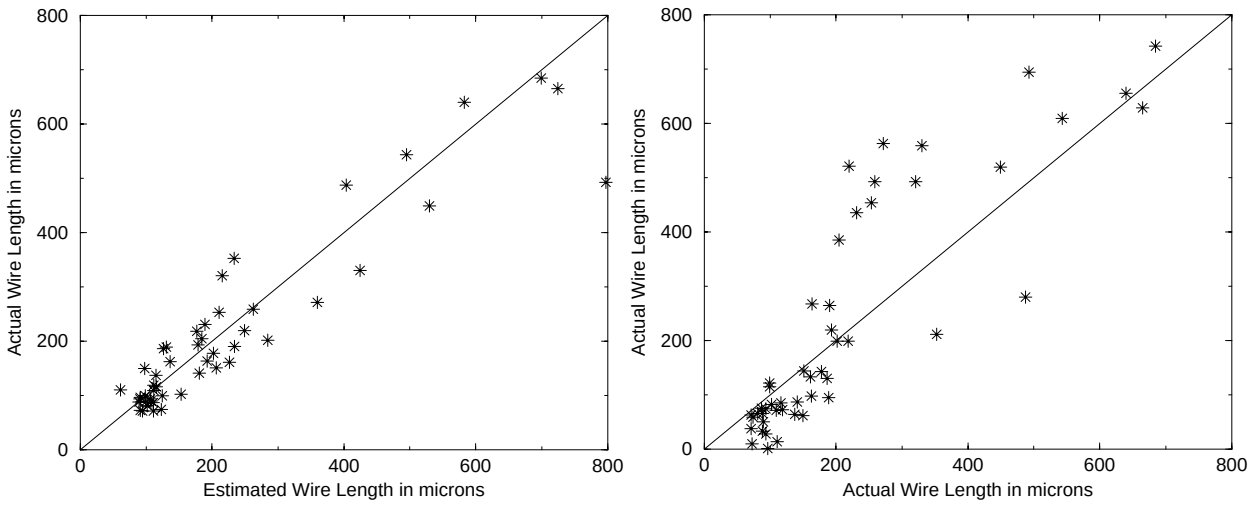

(a) (b)

Figure 7.3 For apex6o, (a) actual vs. estimated wire length using WLE, and (b) inherent noise in the actual wire length.

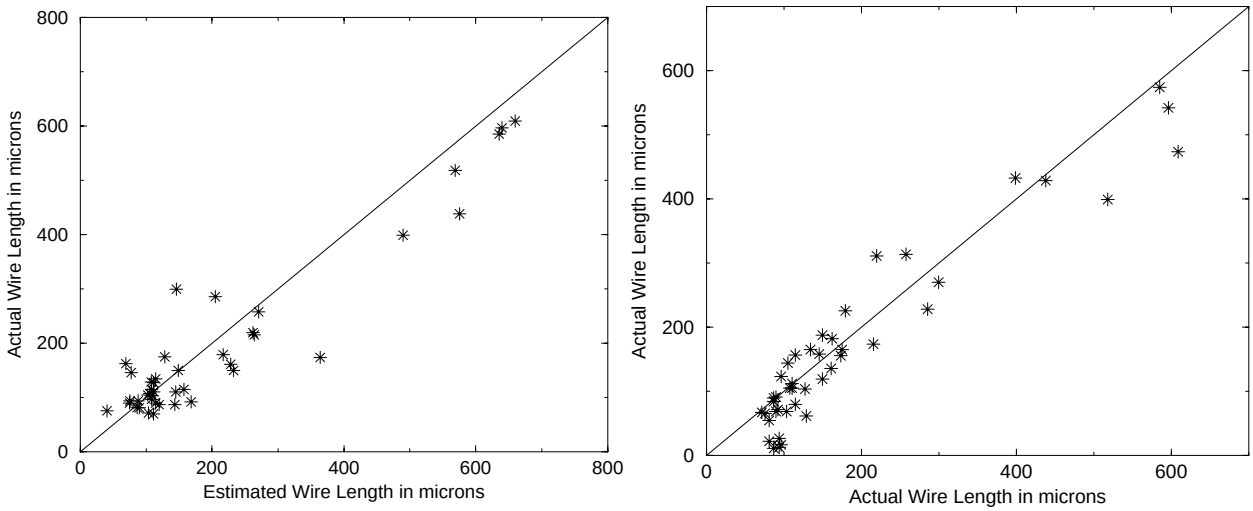

(a) (b)

Figure 7.4 For frg2o, (a) actual vs. estimated wire length using WLE, and (b) inherent noise in the actual wire length.

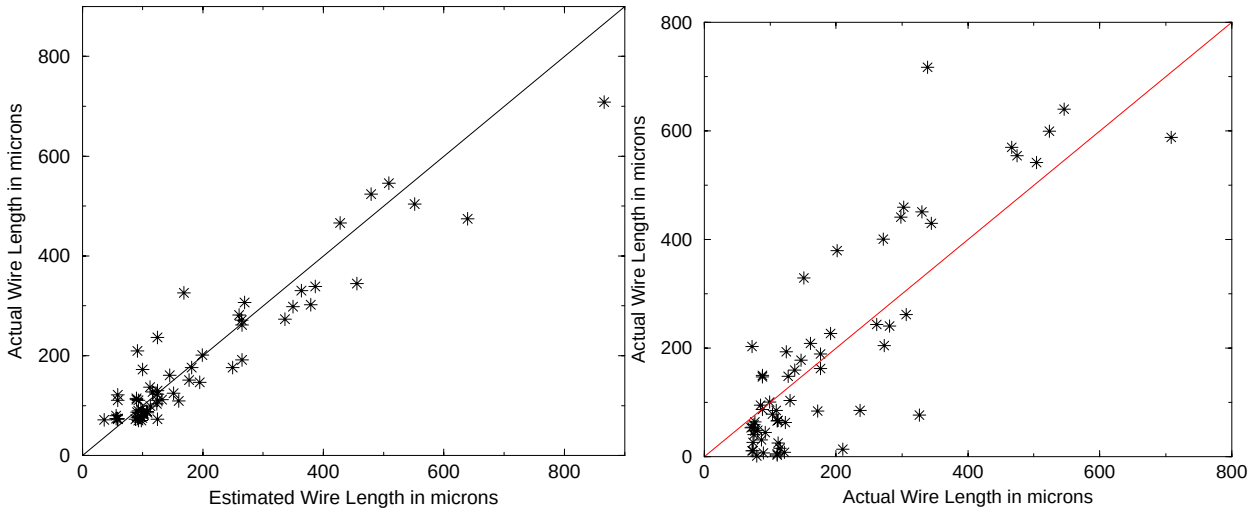

(a) (b)

Figure 7.5 For x3o, (a) actual vs. estimated wire length using WLE, and inherent noise in the (b) actual wire length.

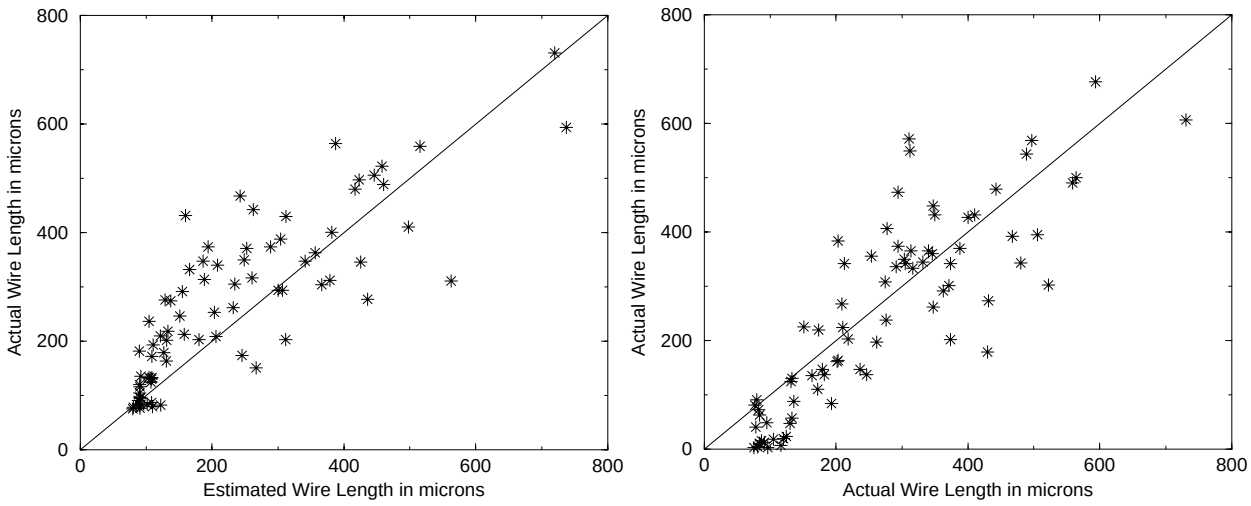

(a) (b)

Figure 7.6 For random10, (a) actual vs. estimated wire length using WLE, and (b) inherent noise in the actual wire length.

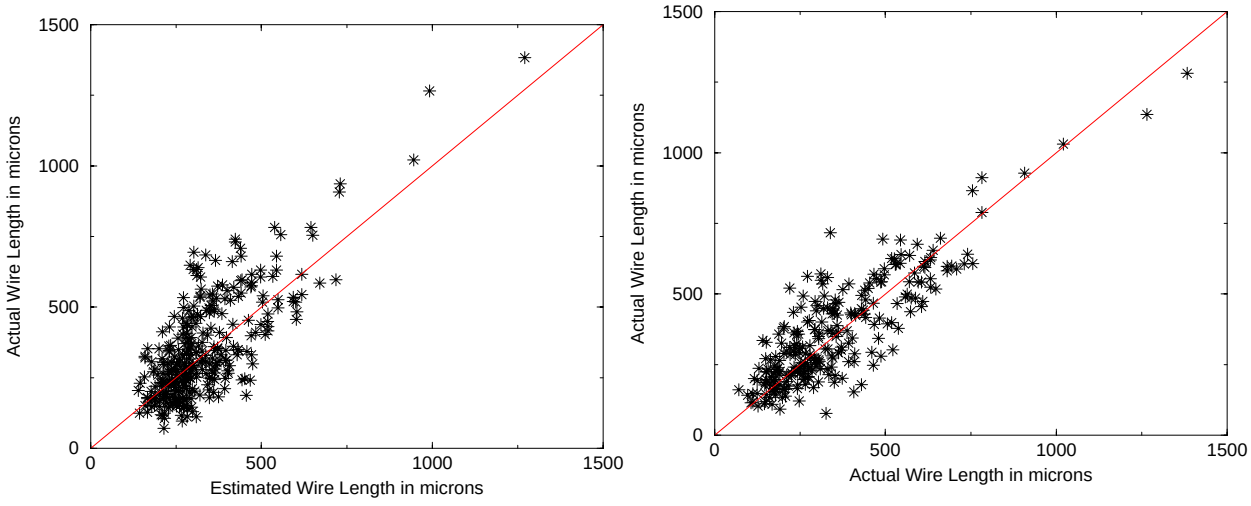

(a) (b)

Figure 7.7 (a) Actual vs.. estimated wire length for long wires using Bounding Box technique, and (b) inherent Noise in the actual wire length.

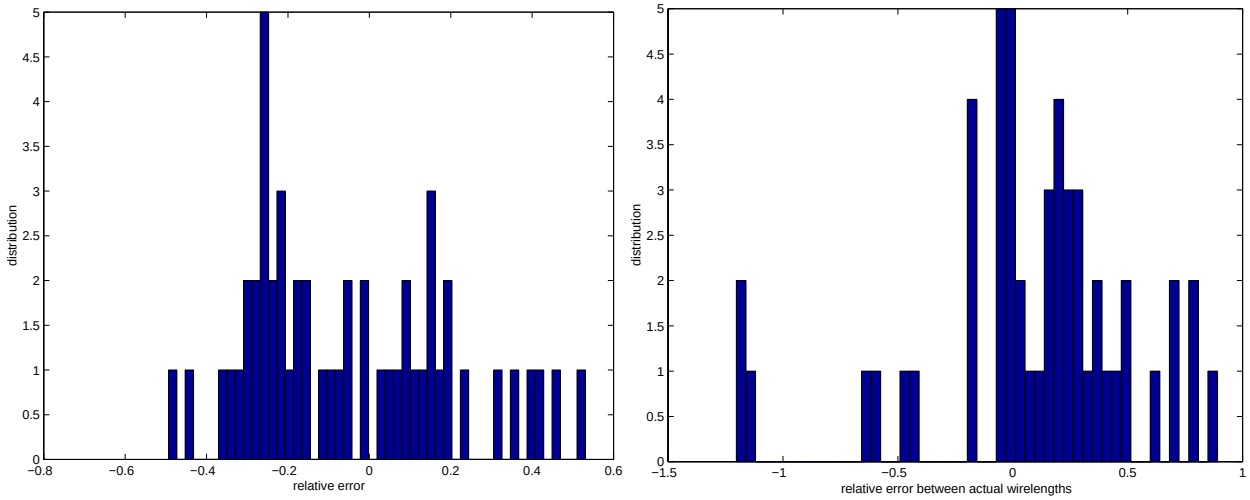

(a) (b)

Figure 7.8 For alu2o, (a) relative error distribution between actual and predicted wirelength, and (b) relative difference between actual wire lengths, due to noise.

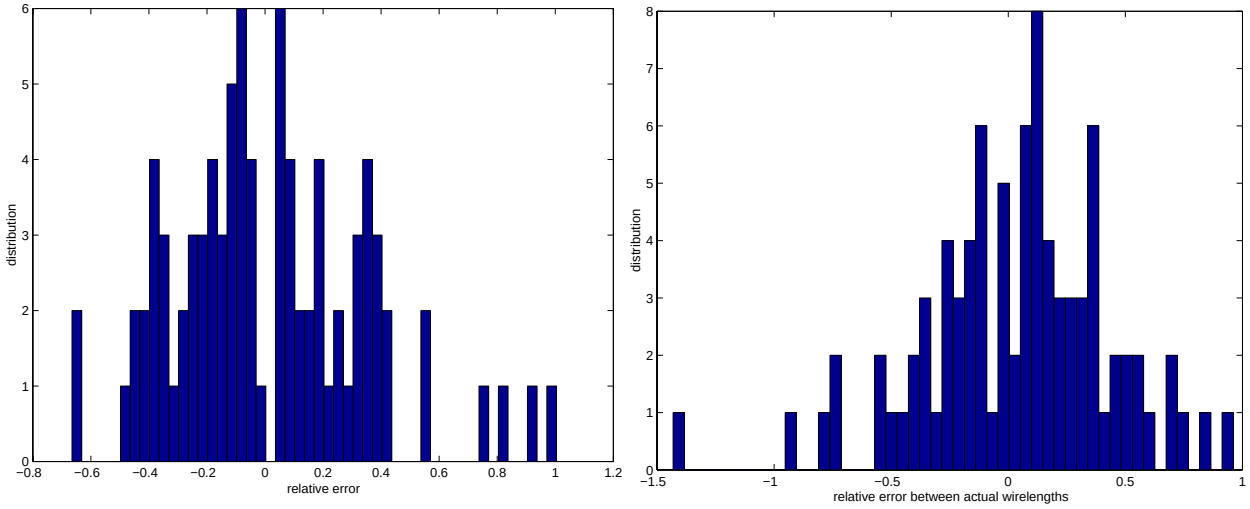

(a) (b)

Figure 7.9 For s1238o, (a) relative error distribution between actual and predicted wirelength, and (b) relative difference between actual wire lengths, due to noise.

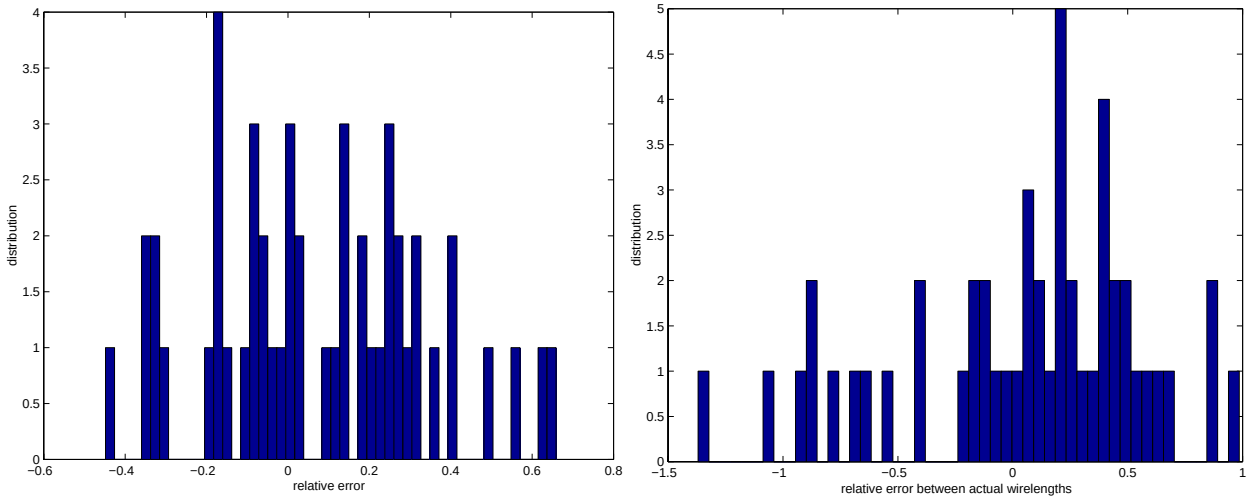

(a) (b)

Figure 7.10 For apex6o, (a) relative error distribution between actual and predicted wirelength, and (b) relative difference between actual wire lengths, due to noise.

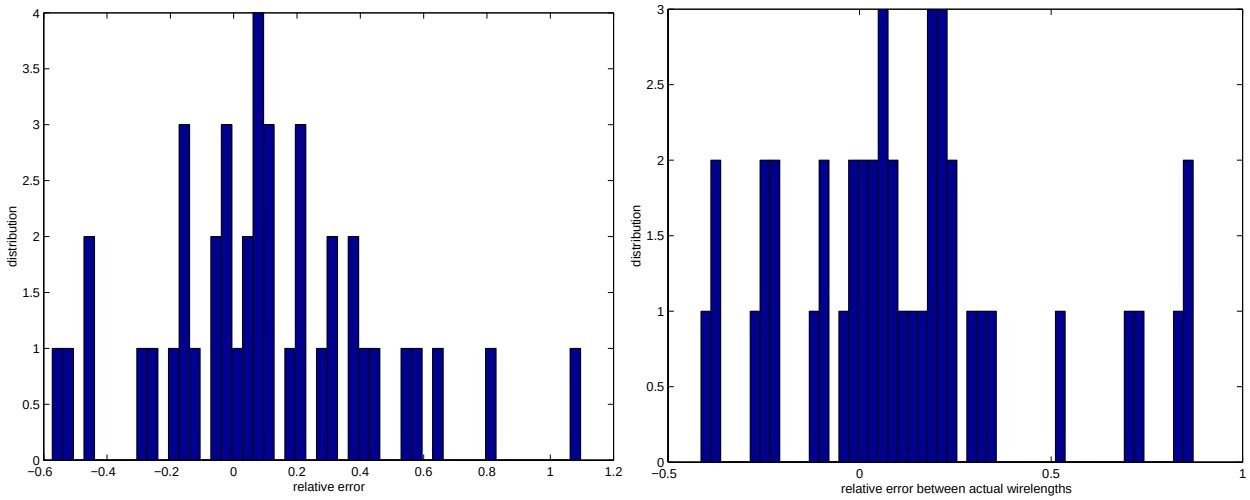

(a) (b)

Figure 7.11 For frg2o, (a) relative error distribution between actual and predicted wirelength, and (b) relative difference between actual wire lengths, due to noise.

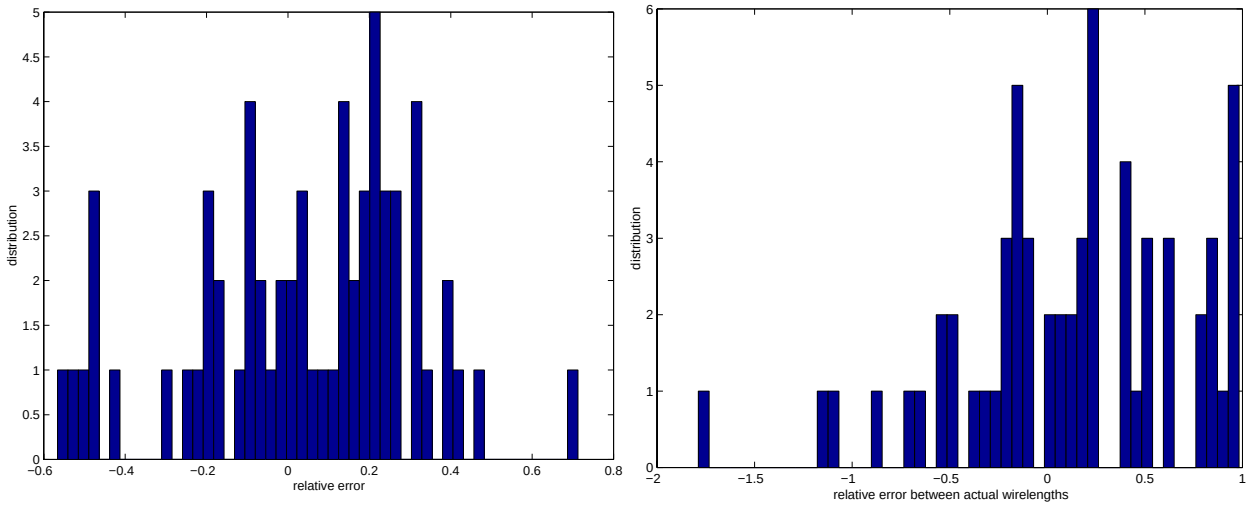

(a) (b)

Figure 7.12 For x3o, (a) relative error distribution between actual and predicted wirelength, and (b) relative difference between actual wire lengths, due to noise.

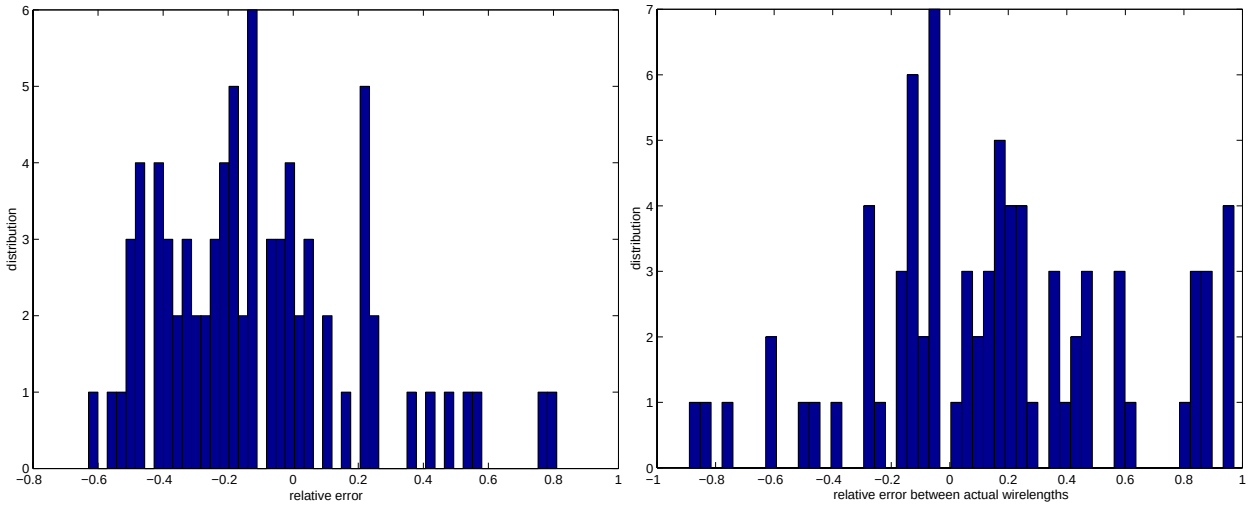

(a) (b)

Figure 7.13 For random10, (a) relative error distribution between actual and predicted wirelength, and (b) relative difference between actual wire lengths, due to noise.

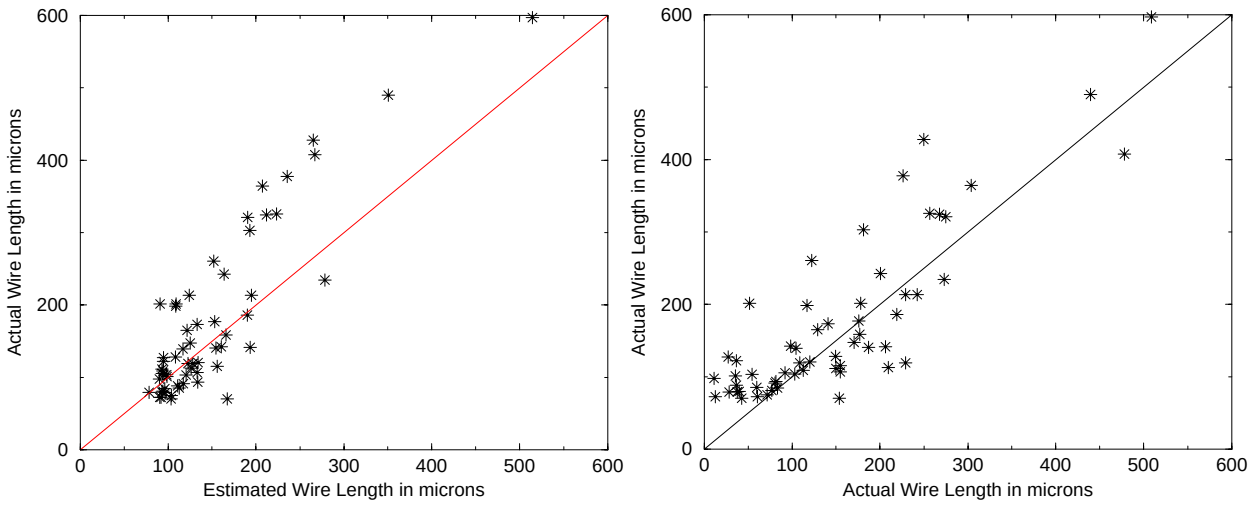

(a) (b)

Figure 7.14 For alu2o (with different library), (a) actual vs. estimated wire length using WLE, and (b) inherent noise in the actual wire length.

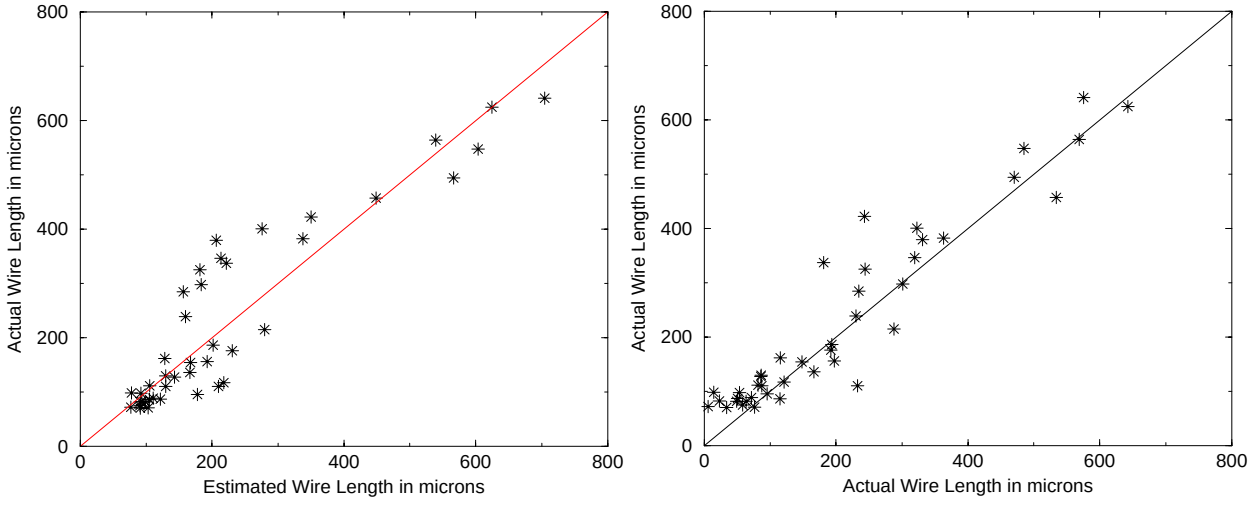

(a) (b)

Figure 7.15 For apex6o (with different library), (a) actual vs. estimated wire length using WLE, and (b) inherent noise in the actual wire length.

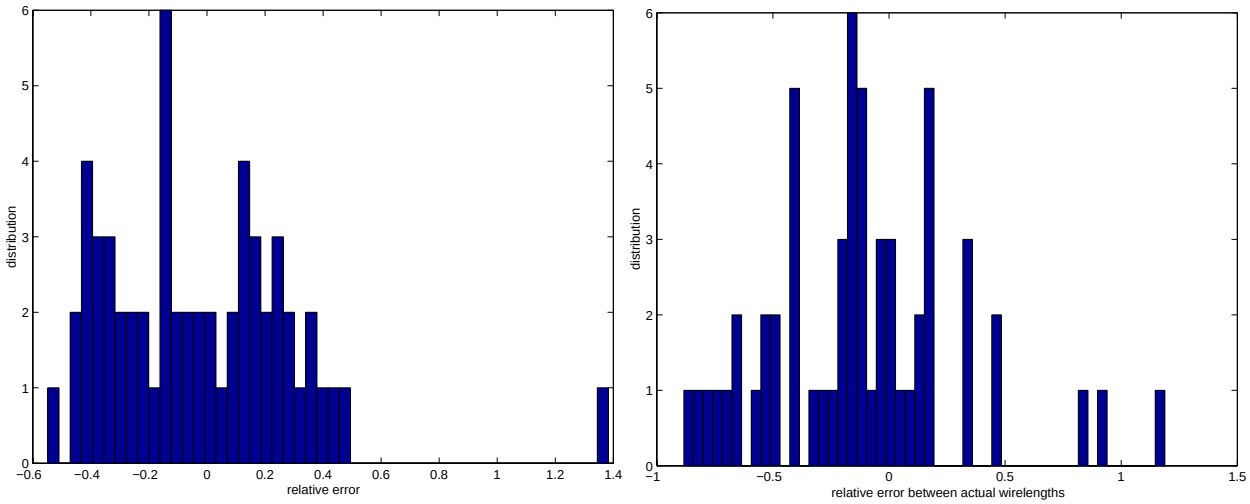

(a) (b)

Figure 7.16 For alu2o (with different library), (a) relative error distribution between actual and predicted wirelength, and (b) relative difference between actual wire lengths, due to noise.

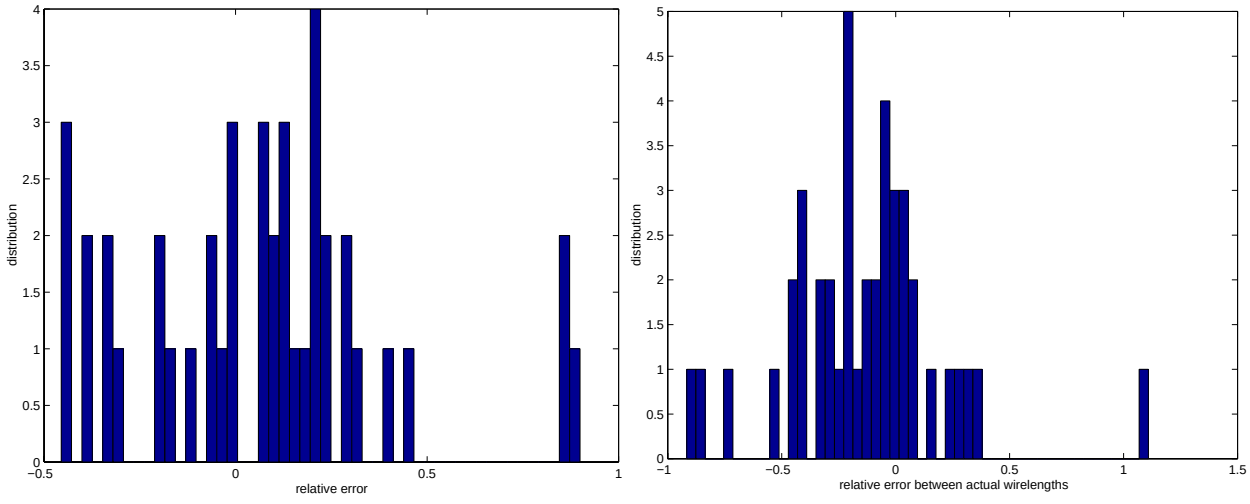

(a) (b)

Figure 7.17 For apex6o (with different library), (a) relative error distribution between actual and predicted wirelength, and (b) relative difference between actual wire lengths, due to noise.